

Effects of counter-rotating-wave terms of the driving field on the spectrum of resonance fluorescence

Yiying Yan, Zhiguo Lü, and Hang Zheng

Key Laboratory of Artificial Structures and Quantum Control (Ministry of Education), Department of Physics and Astronomy, Shanghai Jiao Tong University, Shanghai 200240, China

(Received 3 August 2013; published 15 November 2013)

We investigate the fluorescence spectrum of a two-level system driven by a monochromatic classical field by the Born-Markovian master equation based on a unitary transformation. The main purpose is to understand the effects of counter-rotating-wave terms of the driving on spectral features of the fluorescence. We have derived an analytical expression for the fluorescence spectrum, which is different from Mollow's theory, while Mollow's result on resonance is the limiting case of ours in moderately weak driving regimes. Our results demonstrate precisely that the counter-rotating-wave terms of the driving play an important role in the fluorescence spectrum for intense driving: (i) the counter-rotating coupling suppresses the red sideband in the Mollow triplet and it enhances the blue one in explicitly contrast to the well-known equal intensity of the sideband in Mollow's theory, (ii) the higher-order Mollow triplets appear as a characteristic spectral feature arising from counter-rotating-wave terms of the driving, and (iii) a significant frequency shift of the sidebands is observed, which depends on both the detuning and driving strength.

DOI: [10.1103/PhysRevA.88.053821](https://doi.org/10.1103/PhysRevA.88.053821)

PACS number(s): 42.50.Ct, 42.50.Hz, 32.50.+d, 32.80.-t

I. INTRODUCTION

Mollow initially derived the resonance fluorescence spectrum of a driven two-level system (TLS) [1]. The predicted resonance fluorescence spectrum has been verified in traditional quantum optical experiments [2]. In Mollow's theory, the line shape of the resonance fluorescence spectrum depends on both the TLS spontaneous decay rate and the driving strength. Specifically speaking, the decay rate influences the full width at half maximum (FWHM) of peaks in the spectrum, and the driving strength determines the splitting. For weak driving strengths, the resonance fluorescence spectrum is made up of a single Lorentzian spontaneous emission line. For moderately strong driving strengths, instead of the single Lorentzian line, it consists of three split peaks known as the Mollow triplet.

Recently, there has been increasing experimental investigation of the fluorescence spectrum in artificial atoms, for instance, semiconductor quantum dots [3–9], single molecules [10], and superconducting circuits [11]. The experiments are not only to test fundamental theory but also to develop single-quantum emitters for quantum light spectroscopy and quantum information applications. It is reported in Ref. [11] that the observed fluorescence spectrum is in quantitative agreement with the predictions from Mollow's theory. According to Ref. [9], an individual Mollow sideband channel of the resonance fluorescence from a single quantum dot can act as an efficient single-photon source. However, so far most resonance fluorescence observed in experiments is under conditions such that the driving strength is of the magnitude of the spontaneous decay rate, which is far less than the bare transition frequency of the TLS. Thus, it is not surprising that the theory is consistent with the data from experiments such as that in Ref. [11].

Apart from the experimental research on the fluorescence spectrum, theoretical investigations, which are attractive and significant, can be roughly grouped into two categories. One is studying the influence of the various types of driving and environments in which TLSs exist on the fluorescence spectrum within the rotating-wave approximation (RWA) of driving, such as the works concerning the resonance spectrum

of a quantum dot excited by a strong optical pulse [12] and the influence from a solid-state environment [13]. The other is extending the theory out of the framework of the RWA of driving, such as the work carried out in Ref. [14], the main idea of which is treating the counter-rotating (CR) wave terms of the driving as perturbation in the so-called dressed basis. In intense-driving regimes and on resonance, based on perturbation calculation, the authors found unequally intense sidebands, generation of higher-order Mollow triplets with intensities comparable to those of the first, and an analytical expression for the shift of sidebands in frequency [14].

Although the RWA-based theory succeeds in explaining classical fluorescence experiments, we believe that it is necessary to take into account the effects of CR-wave terms of driving on the same footing as the rotating-wave terms for the following reasons. On the one hand, the RWA loses its validity when the driving strength is comparable to the magnitude of the bare transition frequency of the TLS and/or the driving frequency is detuned from the resonance. The experiments in strongly driven TLS reported in Refs. [15,16] reveal that theories beyond the RWA are needed to explain the observed phenomena. In this work, we show clearly that for a finite-detuning case the spectrum without the RWA differs from the one with the RWA even in weak-driving regimes. On the other hand, the CR-wave terms have important effects on the coherently strongly driven dynamics of the TLS [17,18], such as the intriguing phenomenon known as coherent destruction of tunneling (CDT) [19]. Thus, one can expect that the CR-wave terms should introduce some characteristic spectral features of the scattered light from TLSs in intense-driving regimes.

In this paper, we consider the effects of the CR-wave terms of the driving on fluorescence from a TLS driven by a monochromatic classical field. We take into account the CR-wave terms of driving by means of the same unitary transformation as that of Ref. [20], which has been used to study the coherently driven dynamics of the TLS. Using the unitary transformation, we obtain an effective Hamiltonian

with RWA form, but the corresponding parameters become renormalized, which includes the effects of the CR-wave terms of the driving. From the effective Hamiltonian, it is convenient to calculate the fluorescence spectrum by Mollow's method (Sec. III). In this sense our method is as simple as the RWA method. On the other hand, our previous work shows that the method properly takes into account the CR-wave terms [20]. Using the effective Rabi frequency given in terms of the renormalized parameters, we have calculated the well-known Bloch-Siegert shift up to fourth order of the driving strength, which is exactly the same as the prediction of Floquet theory [21]. In this work we demonstrate the spectral features arising from the CR-wave terms of the driving in three aspects: (i) the asymmetry of the sidebands with respect to the central peak, (ii) the generation of the higher-order Mollow triplets, and (iii) frequency shifts of the sidebands. We discuss these characters and the difference from other works in the Secs. III A and III B.

II. UNITARY TRANSFORMATION AND MASTER EQUATION

The Hamiltonian describing a TLS driven by a classical monochromatic field with the frequency ω_L in a vacuum electromagnetic field reads ($\hbar = 1$)

$$H(t) = \frac{1}{2}\omega_0\sigma_z + \Omega \cos(\omega_L t)\sigma_x + \sum_k \omega_k b_k^\dagger b_k + \frac{1}{2} \sum_k g_k (b_k^\dagger + b_k)\sigma_x, \quad (1)$$

where σ_x and σ_z are Pauli matrices describing the TLS. ω_0 is the bare transition frequency between the two levels, Ω is the driving strength, b_k (b_k^\dagger) is the annihilation (creation) operator of the k th-mode electromagnetic field with frequency ω_k , and g_k is the coupling between the TLS and the k th-mode electromagnetic field.

In order to take into account the CR-wave terms of the driving, we perform a unitary transformation proposed in Ref. [20]. The generator of the unitary transformation is given by

$$S(t) = i \frac{\Omega}{\omega_L} \zeta \sin(\omega_L t)\sigma_x, \quad (2)$$

where we introduce a parameter ζ to be determined later. The transformation $H'(t) = e^{S(t)} H(t) e^{-S(t)} - i e^{S(t)} \frac{d}{dt} e^{-S(t)}$ can be done to the end and yields

$$H'(t) = \frac{1}{2}\omega_0 \cos \left[\frac{2\Omega}{\omega_L} \zeta \sin(\omega_L t) \right] \sigma_z + \frac{1}{2}\omega_0 \sin \left[\frac{2\Omega}{\omega_L} \zeta \sin(\omega_L t) \right] \sigma_y + \Omega(1 - \zeta) \cos(\omega_L t)\sigma_x + \sum_k \omega_k b_k^\dagger b_k + \frac{1}{2} \sum_k g_k (b_k^\dagger + b_k)\sigma_x. \quad (3)$$

Using the identity given in Ref. [22],

$$\exp(iz \sin \theta) = \sum_{n=-\infty}^{\infty} J_n(z) \exp(in\theta), \quad (4)$$

where $J_n(z)$ is a Bessel function of the first kind, we divide the transformed Hamiltonian into two parts,

$$H'(t) = H'_0(t) + H'_1(t), \quad (5)$$

$$H'_0(t) = \frac{1}{2}\omega_0 J_0 \left(\frac{2\Omega}{\omega_L} \zeta \right) \sigma_z + \omega_0 J_1 \left(\frac{2\Omega}{\omega_L} \zeta \right) \sin(\omega_L t)\sigma_y + \Omega(1 - \zeta) \cos(\omega_L t)\sigma_x + \sum_k \omega_k b_k^\dagger b_k + \frac{1}{2} \sum_k g_k (b_k^\dagger + b_k)\sigma_x, \quad (6)$$

$$H'_1(t) = \omega_0 \sum_{n=1}^{\infty} J_{2n+1} \left(\frac{2\Omega}{\omega_L} \zeta \right) \sin[(2n+1)\omega_L t]\sigma_y + \omega_0 \sum_{n=1}^{\infty} J_{2n} \left(\frac{2\Omega}{\omega_L} \zeta \right) \cos(2n\omega_L t)\sigma_z. \quad (7)$$

Up to now, the treatment is exact without any approximation. To proceed, we first introduce an approximation where we drop $H'_1(t)$ because the higher-order harmonic terms ($n\omega_L, n \geq 2$) are negligible according to Ref. [20].

Since our interest is the spectral features of the fluorescence arising from the CR-wave terms of the driving, we assume an RWA for the TLS-environment interaction as Mollow did [1]. This is the second approximation we introduce in the following. To derive the master equation, we further assume weak TLS-environment coupling and the Born-Markovian approximation as usual [23]. These are all the approximations we use for deriving the master equation in this work. If the parameter ζ is determined as

$$\Omega(1 - \zeta) = \omega_0 J_1 \left(\frac{2\Omega}{\omega_L} \zeta \right) \equiv \frac{\tilde{\Omega}}{2}, \quad (8)$$

we obtain our reformulated rotating-wave Hamiltonian,

$$H'(t) = \frac{1}{2}\omega_0 J_0 \left(\frac{2\Omega}{\omega_L} \zeta \right) \sigma_z + \frac{\tilde{\Omega}}{2} (e^{i\omega_L t} \sigma_- + e^{-i\omega_L t} \sigma_+) + \sum_k \omega_k b_k^\dagger b_k + \frac{1}{2} \sum_k g_k (b_k^\dagger \sigma_- + b_k \sigma_+), \quad (9)$$

where $\sigma_{\pm} = \frac{1}{2}(\sigma_x \pm i\sigma_y)$. We perform the unitary rotating transformation given by

$$R(t) = \exp \left[i\omega_L t \left(\frac{1}{2}\sigma_z + \sum_k b_k^\dagger b_k \right) \right], \quad (10)$$

then obtain a time-independent Hamiltonian,

$$\begin{aligned} \tilde{H} &= R(t)H'(t)R^\dagger(t) + i \frac{\partial R(t)}{\partial t} R^\dagger(t) \\ &= \frac{1}{2}(\tilde{\delta}\sigma_z + \tilde{\Omega}\sigma_x) + \sum_k (\omega_k - \omega_L) b_k^\dagger b_k \\ &\quad + \frac{1}{2} \sum_k g_k (b_k^\dagger \sigma_- + b_k \sigma_+) \\ &\equiv \tilde{H}_{0S} + \tilde{H}_{0B} + \tilde{H}_1, \end{aligned} \quad (11)$$

where the effective detuning $\tilde{\delta} = \omega_0 J_0(\frac{2\Omega}{\omega_L} \zeta) - \omega_L$, \tilde{H}_{0S} is the dressed TLS-driving Hamiltonian, \tilde{H}_{0B} is the environment

term, and \tilde{H}_1 is the TLS-environment coupling. Provided the Born-Markovian approximation is used in the derivation of the master equation in the rotating basis, the master equation for the reduced density matrix of the TLS, $\tilde{\rho}_S(t) = \text{Tr}_B[\tilde{\rho}_{SB}(t)]$, takes the same form as Mollow's:

$$\frac{d}{dt}\tilde{\rho}_S(t) = -i[\tilde{H}_{0S}, \tilde{\rho}_S(t)] - \frac{\kappa}{2}[\sigma_+\sigma_-\tilde{\rho}_S(t) + \tilde{\rho}_S(t)\sigma_+\sigma_- - 2\sigma_-\tilde{\rho}_S(t)\sigma_+], \quad (12)$$

where the subscript S denotes the TLS and κ is the spontaneous decay rate of the TLS. The derivation of the master equation is given in Appendix A.

According to Eq. (12), it is easy to obtain the Bloch equations, which take the form

$$\frac{d}{dt} \begin{pmatrix} \langle \sigma_+(t) \rangle \\ \langle \sigma_-(t) \rangle \\ \langle \sigma_z(t) \rangle \end{pmatrix} = \begin{pmatrix} -\frac{\kappa}{2} + i\tilde{\delta} & 0 & -i\frac{\tilde{\Omega}}{2} \\ 0 & -\frac{\kappa}{2} - i\tilde{\delta} & i\frac{\tilde{\Omega}}{2} \\ -i\tilde{\Omega} & i\tilde{\Omega} & -\kappa \end{pmatrix} \begin{pmatrix} \langle \sigma_+(t) \rangle \\ \langle \sigma_-(t) \rangle \\ \langle \sigma_z(t) \rangle \end{pmatrix} + \begin{pmatrix} 0 \\ 0 \\ -\kappa \end{pmatrix}. \quad (13)$$

Here, $\langle \sigma_\mu(t) \rangle = \text{Tr}[\tilde{\rho}_S(t)\sigma_\mu]$, ($\mu = +, -, z$). The equations have the steady-state solutions

$$\langle \sigma_+ \rangle_s = \langle \sigma_- \rangle_s^* = \frac{-\tilde{\Omega}(2\tilde{\delta} - i\kappa)}{2\tilde{\Omega}^2 + 4\tilde{\delta}^2 + \kappa^2}, \quad (14)$$

$$\langle \sigma_z \rangle_s = \frac{-4\tilde{\delta}^2 - \kappa^2}{2\tilde{\Omega}^2 + 4\tilde{\delta}^2 + \kappa^2}. \quad (15)$$

These results show that the solutions depend on the effective detuning and modified driving strength. If we do not apply the unitary transformation but assume the RWA for the driving and follow the same procedure from Eq. (10) to (12), we obtain the same differential equation without modified driving strength and detuning. In other words, the parameters in the above equations are replaced as follows:

$$\tilde{\Omega} \rightarrow \Omega, \quad \tilde{\delta} \rightarrow \delta = \omega_0 - \omega_L, \quad (16)$$

and they become the results of Mollow's master equation [1].

III. FLUORESCENCE SPECTRUM

In general, the power spectrum of the scattered light is obtained from the time-integrated Fourier transformation of the first-order correlation function [24],

$$S(\omega) = \frac{1}{2\pi} \lim_{T \rightarrow \infty} \frac{1}{T} \int_0^T dt \int_0^T dt' g^{(1)}(t, t') e^{-i\omega(t-t')}, \quad (17)$$

where the correlation function $g^{(1)}(t, t') = \langle U^\dagger(t)\sigma_+U(t)U^\dagger(t')\sigma_-U(t') \rangle$, with $U(t)$ being the evolution operator for the original Hamiltonian. We analytically derive the fluorescence spectrum in Appendix B.

The fluorescence spectrum consists of the so-called coherent (Rayleigh scattering) and incoherent (inelastic scattering) components. The coherent one arising from the term $\langle \sigma_\mu(\tau \rightarrow \infty)\sigma_\nu(0) \rangle$ is the δ function,

$$S_c(\omega) = \frac{1}{4\pi} \sum_{n \text{ odd}} I_{n,0} \delta(\omega - n\omega_L), \quad (18)$$

with

$$I_{n,0} = (j_n^2 + j_{n+2}^2) |\langle \sigma_+ \rangle_s|^2 + j_n j_{n+2} (\langle \sigma_- \rangle_s^2 + \langle \sigma_+ \rangle_s^2) + (j_n j_{n+1} + j_{n+1} j_{n+2}) \times \langle \sigma_z \rangle_s (\langle \sigma_- \rangle_s + \langle \sigma_+ \rangle_s) + j_{n+1}^2 \langle \sigma_z \rangle_s^2, \quad (19)$$

where the summation is taken over all positive odd integers and coefficients j_n and j'_n have been defined in Appendix B. We denote the roots of the third-degree polynomial (B12), $f(p)$, by $-\gamma_1$ and $-\gamma_2 \pm i\Omega'$. Then the incoherent part of the spectrum is written as

$$S_{\text{inc}}(\omega) = \frac{1}{4\pi} \text{Re} \sum_{n \text{ odd}} \left[I_{n,1} \frac{\gamma_1 + i(n\omega_L - \omega)}{\gamma_1^2 + (\omega - n\omega_L)^2} + I_{n,2} \frac{\gamma_2 + i(n\omega_L - \Omega' - \omega)}{\gamma_2^2 + (\omega - n\omega_L + \Omega')^2} + I_{n,3} \frac{\gamma_2 + i(n\omega_L + \Omega' - \omega)}{\gamma_2^2 + (\omega - n\omega_L - \Omega')^2} + I'_{n,1} \frac{\gamma_1 - i(n\omega_L + \omega)}{\gamma_1^2 + (\omega + n\omega_L)^2} + I'_{n,2} \frac{\gamma_2 - i(n\omega_L + \Omega' + \omega)}{\gamma_2^2 + (\omega + n\omega_L + \Omega')^2} + I'_{n,3} \frac{\gamma_2 - i(n\omega_L - \Omega' + \omega)}{\gamma_2^2 + (\omega + n\omega_L - \Omega')^2} \right], \quad (20)$$

with

$$I_{n,l} = j_n^2 R_{+,l}^{(-)} + j_n j_{n+2} R_{-,l}^{(-)} + j_n j_{n+1} R_{z,l}^{(-)} + j_n j_{n+2} R_{+,l}^{(+)} + j_{n+2}^2 R_{-,l}^{(+)} + j_{n+1} j_{n+2} R_{z,l}^{(+)} + j_n j_{n+1} R_{+,l}^{(z)} + j_{n+1} j_{n+2} R_{-,l}^{(z)} + j_{n+1}^2 R_{z,l}^{(z)}, \quad (21)$$

$$I'_{n,l} = j_{n+2}^2 R_{+,l}^{(-)} + j'_n j_{n+2} R_{-,l}^{(-)} + j_{n+1} j_{n+2} R_{z,l}^{(-)} + j'_n j_{n+2} R_{+,l}^{(+)} + j_n^2 R_{-,l}^{(+)} + j'_n j_{n+1} R_{z,l}^{(+)} + j_{n+1} j_{n+2} R_{+,l}^{(z)} + j'_n j_{n+1} R_{-,l}^{(z)} + j_{n+1}^2 R_{z,l}^{(z)}. \quad (22)$$

The quantities in Eqs. (21) and (22) are defined and evaluated in Appendix B.

Up to now, we have obtained the modified spectrum, which takes a more complex form than Mollow's. The expression indicates that there are higher-order Mollow triplets, the central peaks of which locate at odd multiples of the driving frequency $n\omega_L$. These higher-order triplets fail to be captured with the RWA for the driving and are consistent with the predictions from the previous works based on different methods [14,25]. In Eq. (20), the last three terms in the square brackets are the additional terms arising from the CR-wave terms.

A. Spectral features and effects of the CR-wave terms

In the following, we illustrate precisely the spectral features induced by the CR-wave terms. We set the bare transition frequency ω_0 as the unit. At the same time, we only show the incoherent part of the fluorescence in the plots.

To begin with, we examine whether the fluorescence spectrum on resonance obtained from our method coincides with Mollow's when the driving strength is moderately weak. We show the spectrum on resonance for driving strength

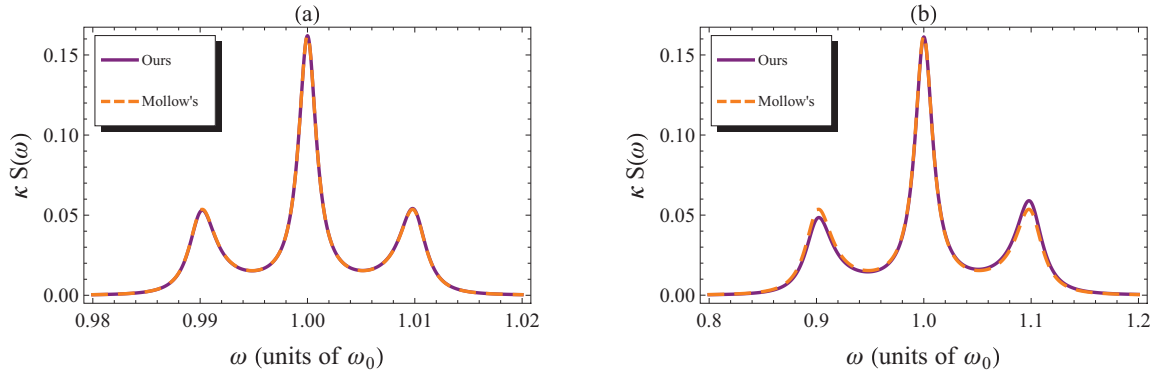


FIG. 1. (Color online) The resonance fluorescence spectrum as a function of frequency ω for $\Omega = 5\kappa$ and (a) $\Omega/\omega_0 = 0.01$ and (b) $\Omega/\omega_0 = 0.1$. The solid line represents our spectrum, and the dashed line shows Mollow's spectrum.

$\Omega = 5\kappa$ with $\Omega/\omega_0 = 0.01, 0.1$ in Figs. 1(a) and 1(b), respectively. It turns out that under the moderately weak driving strength and resonance condition, the spectrum calculated by our method is in good agreement with Mollow's. However, when $\Omega/\omega_0 = 0.1$, our calculated spectrum is slightly different from Mollow's because it has a higher blue sideband and a lower red sideband compared with Mollow's. These results indicate that the effects of CR-wave terms are negligible under the weak driving strength and resonance condition. The effects of driving CR terms become clearer with increasing driving strength. Therefore, the RWA-based theory is adequate and succeeds in explaining classical fluorescence experiments.

We now illustrate the influence of the CR-wave terms on the line shape of the fluorescence spectrum when increasing

driving strength to the magnitude comparable to the bare transition frequency. In Figs. 2(a)–2(c), we plot the spectrum as a function of frequency ω for $\Omega = 10\kappa$ and $\Omega/\omega_0 = 0.6$ with the three detuning values $\delta/\omega_0 = 0.2, 0, -0.2$, respectively. The asymmetry of the two sidebands with respect to the central peak for $\Omega/\omega_0 = 0.6$ becomes noticeable. Comparing our results with Mollow's results in Figs. 2(a)–2(c), we notice the common character that the red sideband of our calculated spectrum is suppressed while the blue sideband is enhanced. Furthermore, Fig. 3 shows that this effect can be strengthened by increasing the driving strength. Moreover, our theory predicts that a significant shift of the two sidebands in frequency can be observed with proper detuning and driving strength. In Fig. 4, we show the second Mollow triplet, whose

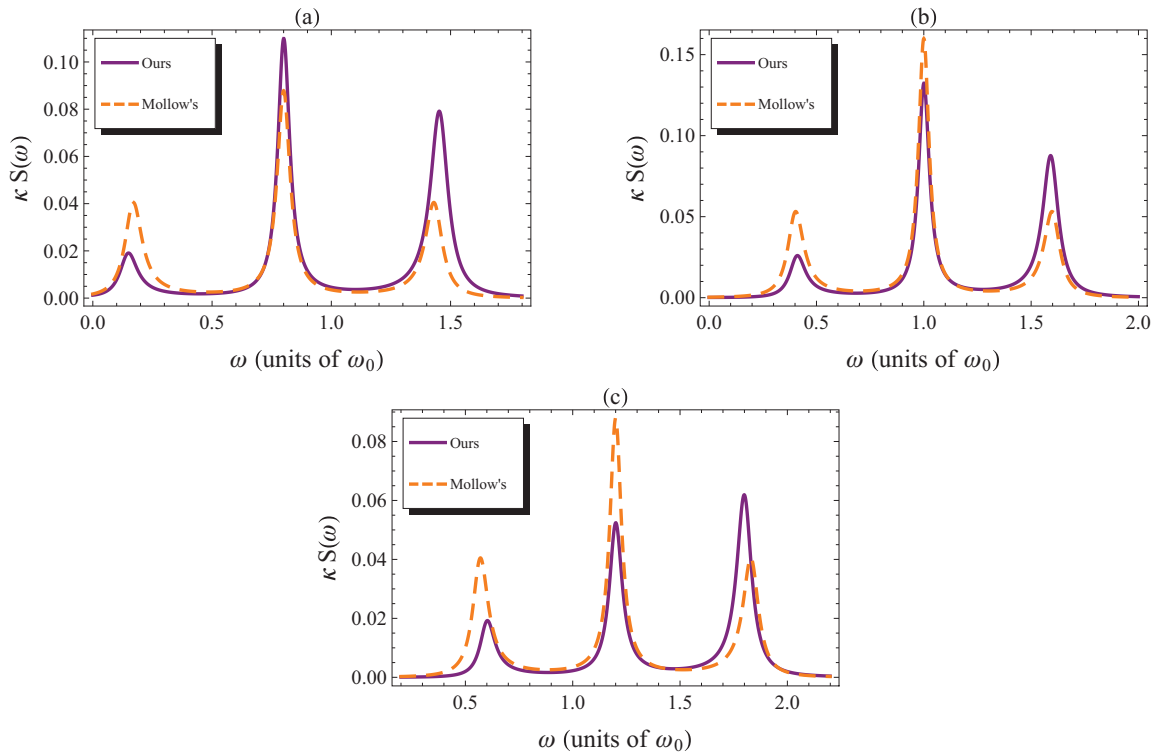


FIG. 2. (Color online) The fluorescence spectrum as a function of frequency ω for $\Omega = 10\kappa$, $\Omega/\omega_0 = 0.6$, and (a) $\omega_L = 0.8\omega_0$, (b) $\omega_L = \omega_0$, and (c) $\omega_L = 1.2\omega_0$. The solid line represents our spectrum, and the dashed line shows Mollow's spectrum.

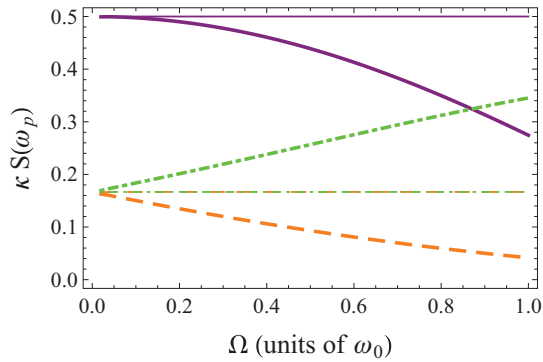


FIG. 3. (Color online) The dimensionless height $\kappa S(\omega_p)$ as a function of driving strength Ω with $\omega_p = \omega_L, \omega_L \mp \Omega'$, corresponding to the central peak (solid line), red sideband (dashed line), and blue sideband (dot-dashed line) in the first triplet. The driving frequency is $\omega_L = \omega_0$, and the decay rate $\kappa = 10^{-3}\omega_0$. All thick lines represent our predictions, and the thin ones are Mollow's predictions.

central peak is at the frequency $\omega = 3\omega_L$ on resonance and $\Omega/\omega_0 = 0.9$. Even for such strong driving, the intensity of the second Mollow triplet is much less than that of the first. This feature of the higher-order triplet is distinguished from that in previous work [14]. Our method demonstrates that the higher-order triplet clearly comes from the counter-rotating term of the driving field which is depicted in Eq. (20), and its intensity is determined by a coefficient with higher-order Bessel functions. Therefore, the experimental study of the higher-order triplet is an interesting challenge.

In Figs. 2, 3, and 4, we show the spectral features arising from the CR-wave terms in three aspects: (i) the asymmetry of the sidebands with respect to the central peak, (ii) the generation of the higher-order Mollow triplets, and (iii) shifts of the sidebands. Although some characters have been reported in previous works [14,25], we identify that there are dramatic differences between our results and those in Ref. [14].

First of all, we clearly show that the CR-wave terms enhance the emission of the red sideband while suppressing

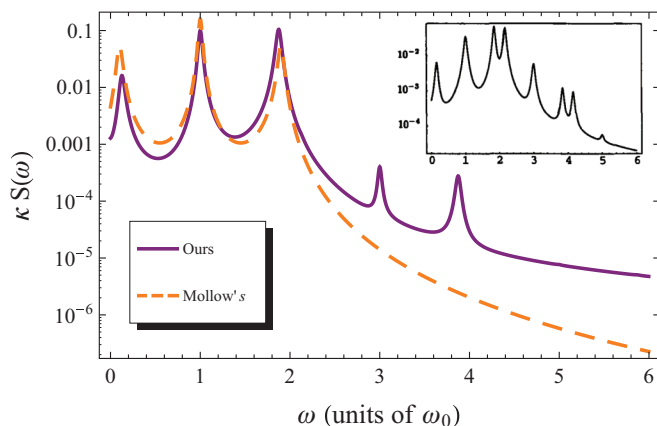


FIG. 4. (Color online) The fluorescence spectrum obtained by our method (solid line) and Mollow's method (dashed line) on a logarithmic scale for $\Omega = 20\kappa$, $\Omega/\omega_0 = 0.9$, and $\omega_L = \omega_0$. The inset shows the spectrum obtained in Ref. [14] with the same parameters.

that of the blue one compared with Mollow's spectra. This feature deterministically comes from the CR-wave terms and is different from the result claimed in Ref. [14], i.e., the unequally intense Mollow sidebands. Since the method in Ref. [14] has taken into account the effects of the three different decay rates, which also cause the unequally intense Mollow sidebands, we believe that the unequally intense Mollow sidebands claimed in Ref. [14] arise from the combined effects of both different decay rates and the CR-wave terms.

Second, our calculations clearly show the higher-order Mollow triplets, which come from the effects of the CR-wave terms. Moreover, the detailed character is distinct from those of Ref. [14]. We find that a higher-order Mollow triplet with very weak intensities relative to the first one, while in Ref. [14] the second Mollow triplet becomes comparable in intensity to the first triplet. We show numerical results with the same parameters as those in Fig. 6 of Ref. [14]. In Fig. 4, it is clearly seen that the magnitudes of the three peaks of the second Mollow triplet are far less than the magnitude of the central line of the first one. The ratio of intensities between the emission lines of the second Mollow triplet and central line of the first triplet is about 1/100 for $\Omega/\omega_0 = 0.9$, which shows the dramatic difference between the results obtained by the two methods (see the inset in Fig. 4). In contrast, the results of Ref. [14] show that the height of the red sideband in the second Mollow triplet is of the same magnitude as the central line in the first triplet for $\Omega/\omega_0 = 0.9$. However, the same sideband in our calculated spectrum almost disappears for this case.

Finally, we show a comparison of the shifts of sidebands relative to Mollow's spectrum predicted by our method and Ref. [14]. In the weak-driving regime, both shifts are almost the same. However, as the driving strength increases from $\Omega/\omega_0 = 0.7$ to 1 [see Fig. 5(b)], the shift obtained in Ref. [14] sharply increases. This probably results from the second-order energy corrections containing a divergent term. As a comparison, the valid parameter space of our method is clearly shown in Fig. 6 in our previous work [20]. Further, the method works very well from the weak driving strength to intermediate strong driving strength in the resonance and near-resonance regimes. Moreover, since the Bloch-Siegert shift obtained by our method is exact up to fourth order, it strongly proves that our method properly takes into account the effects of the CR-wave terms of the driving. Thus, we believe that the shift obtained by our method is reliable.

B. CR-wave terms modulated frequency shift

In the following, we focus on the frequency shift of the sidebands caused by CR-wave terms of the driving which may be detectable in experiment. In a way similar to Mollow's theory, the third-degree polynomial equation [Eq. (B12) in Appendix B], which takes the same form obtained by Mollow but with the corresponding renormalized coefficients, completely determines the FWHM of the fluorescence spectrum, i.e., γ_1 and γ_2 , and the splitting between the central peak and its satellite sidebands, i.e., Ω' . In general, the quantity Ω' determined in Eq. (B12) is different from Mollow's due to the effects of the CR-wave terms. As a result, the sideband's shift in frequency occurs. In order to determine the influence

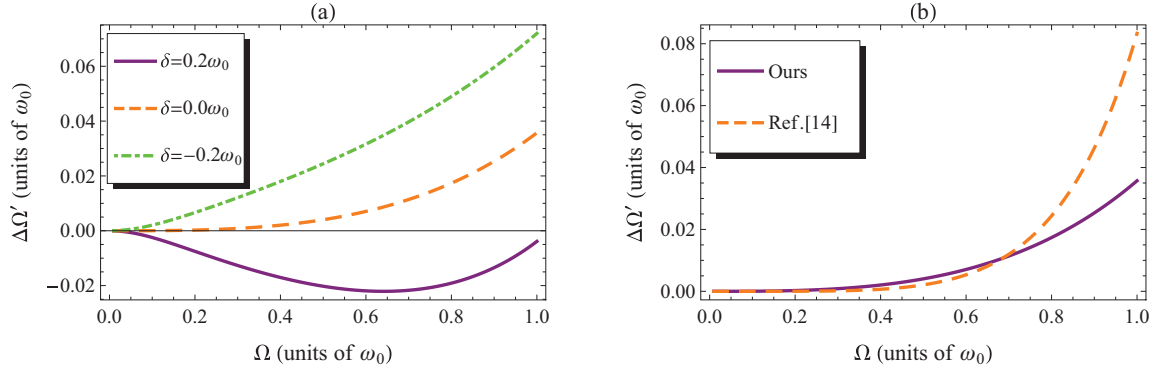


FIG. 5. (Color online) (a) The shift $\Delta\Omega'$ of sidebands as a function of driving strength Ω for $\kappa = 10^{-3}\omega_0$ and various driving frequencies: $\omega_L = 0.8\omega_0$ (solid line), $\omega_L = \omega_0$ (dashed line), and $\omega_L = 1.2\omega_0$ (dot-dashed line). (b) The comparison between the shift obtained in Ref. [14] and ours for the exact resonance and $\kappa = 10^{-3}\omega_0$.

of the CR-wave terms on this frequency shift, we can define the difference $\Delta\Omega' = \Omega'_M - \Omega'$ as a significant frequency shift, where Ω'_M denotes the splitting between the central peak and its sidebands in Mollow's theory. It is known that in the intense-driving limit ($\Omega \gg \kappa$), the splitting Ω'_M is well approximated by the Rabi frequency $\Omega_R = \sqrt{\delta^2 + \Omega^2}$ in Mollow's theory. Thus, the modulated frequency shift due to CR-wave terms can be approximated to the difference $\Omega_R - \tilde{\Omega}_R$ since the effective Rabi frequency $\tilde{\Omega}_R = \sqrt{\tilde{\delta}^2 + \tilde{\Omega}^2}$ in our method has taken into account the effects of the CR-wave terms. It is worth noting that the shift obtained by our method is beyond the second-order corrections [20]. As a comparison, the shift obtained in Ref. [14] results from the second-order energy corrections.

Figure 5 shows how the driving strength affects the shift. $\Delta\Omega' < 0$ means that the sidebands of our prediction shift outwards to the center, $\Delta\Omega' > 0$ means that the sidebands of our prediction shift inwards to the center, and $\Delta\Omega' = 0$ means that the frequencies of the sidebands predicted by the two methods are equal. Since the shift is slight on resonance for weak driving, the RWA is a sufficiently good approximation under such conditions. However, a significant amount of shift emerges when the detuning $\delta = \pm 0.2\omega_0$ even for a small

value of Ω . This indicates that it is necessary to take into account the effects of the CR-wave terms in the off-resonance case where the RWA breaks down even for weak driving strength. When $\delta = 0.2\omega_0$, the absolute value of the effective detuning $\tilde{\delta}$ changes nonmonotonously as Ω increases. As a result, the shift increases slowly at first and then decreases with increasing Ω . Figure 5(b) shows the difference between the shift obtained in Ref. [14] and our result on resonance. In the weak-driving regime, the shifts are almost the same. They rise with increasing Ω . However, when the driving strength increases from $\Omega/\omega_0 = 0.7$ to 1, the shift obtained in Ref. [14] sharply increases, which probably results from the divergent term in the second-order energy correction.

Figure 6 shows the dependence of the shift on the detuning δ for various driving strengths. For $\Omega \ll \omega_0$, the shift is too slight to be observed in the line shape of the spectrum. When Ω is comparable to ω_0 , we notice that a negative detuned driving, i.e., $\omega_L > \omega_0$, is favorable for obtaining a larger shift with a given driving strength. In the intensive-driving regime, one has $\Delta\Omega' = \Omega_R - \tilde{\Omega}_R$. As δ/ω_0 increases from zero to -0.2 in the case $\Omega/\omega_0 = 0.9$, one can verify that the difference between Ω_R and $\tilde{\Omega}_R$ increases monotonically. Thus, the shift increases to a maximum value of $0.06\omega_0$ at $\delta = -0.2\omega_0$. This helps us detect the CR-modified frequency shift in experiment.

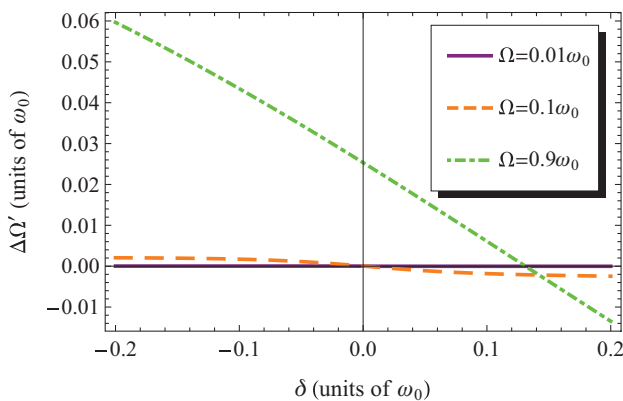


FIG. 6. (Color online) The shift $\Delta\Omega'$ of sidebands as a function of detuning δ for $\Omega = 20\kappa$ and various ratios: $\Omega/\omega_0 = 0.01$ (solid line), $\Omega/\omega_0 = 0.1$ (dashed line), and $\Omega/\omega_0 = 0.9$ (dot-dashed line).

IV. CONCLUSIONS

In summary, we have developed an analytical approach based on a unitary transformation to investigate the spectral features of the scattered light from a two-level system driven by a monochromatic classical field. The method has taken into account the effects of the CR-wave terms of the driving but still retains the simple RWA form of the driving with the CR-modified parameters, which is distinct from the traditional perturbative method. We have derived an analytical expression for the fluorescence spectrum. Our calculated results clearly show the spectral features arising from the CR-wave terms in three aspects: (i) the asymmetry of the sidebands with respect to the central peak, (ii) the generation of the higher-order Mollow triplets, and (iii) shifts of the sidebands. First, since the red sideband is suppressed while the blue sideband is enhanced

in comparison with Mollow's triplet, our calculation shows that the CR-wave term of the driving induces the asymmetry of the sidebands. Second, our theory also predicts the generation of the higher-order Mollow triplets, which is qualitatively consistent with the results of other methods in previous work [14,25]. However, we have found that the intensities of the higher-order Mollow triplets are far less than those of the first triplet. This feature is distinct from that of the previous work. Third, we readily observe that the sidebands in the first triplet shift from the positions of the corresponding sidebands given by Mollow's theory in intense-driving regimes. Moreover, the shift depends on both the driving strength and the detuning. A negative detuning of the driving is favorable for generating a larger shift for a fixed, moderately intense driving strength. We expect that all the effects of the CR-wave terms would be experimentally observable with elaborately designed detuning and driving strength. Our results illustrate that the CR-wave terms of the driving have significant effects on the spectral features of fluorescence.

ACKNOWLEDGMENTS

This work was supported by the National Natural Science Foundation of China (Grants No. 11174198, No. 11374208, and No. 91221201) and the National Basic Research Program of China (Grant No. 2011CB922202).

APPENDIX A: MASTER EQUATION UNDER BORN-MARKOVIAN APPROXIMATION

In the interaction picture of the dressed Hamiltonian, the density matrix satisfies the equation of motion,

$$\frac{d}{dt}\tilde{\rho}_{SB}^I(t) = -i[\tilde{H}_I(t), \tilde{\rho}_{SB}^I(t)], \quad (\text{A1})$$

where $\tilde{\rho}_{SB}^I(t) = e^{i(\tilde{H}_{0S} + \tilde{H}_{0B})t} \tilde{\rho}_{SB}(t) e^{-i(\tilde{H}_{0S} + \tilde{H}_{0B})t}$ and

$$\begin{aligned} \tilde{H}_I(t) &= e^{i(\tilde{H}_{0S} + \tilde{H}_{0B})t} \tilde{H}_I e^{-i(\tilde{H}_{0S} + \tilde{H}_{0B})t} \\ &= e^{i\tilde{H}_{0S}t} \tilde{H}_I(t) e^{-i\tilde{H}_{0S}t}. \end{aligned} \quad (\text{A2})$$

Equation (A1) can be integrated formally and yields

$$\tilde{\rho}_{SB}^I(t) = \tilde{\rho}_{SB}^I(0) - i \int_0^t d\tau [\tilde{H}_I(\tau), \tilde{\rho}_{SB}^I(\tau)]. \quad (\text{A3})$$

Substituting expression (A3) back into Eq. (A1) and taking the trace over the degree of freedom of the environment, we obtain the following equation:

$$\frac{d}{dt}\tilde{\rho}_S^I(t) = -\text{Tr}_B \int_0^t d\tau [\tilde{H}_I(t), [\tilde{H}_I(\tau), \tilde{\rho}_S^I(\tau)\rho_B]], \quad (\text{A4})$$

where we have used the Born approximation $\tilde{\rho}_{SB}^I(\tau) \approx \tilde{\rho}_S^I(\tau)\rho_B$ since in the weak-coupling regime the influence of the system on the environment is negligible. We further introduce Markovian approximation, which assumes $\tilde{\rho}_S^I(\tau) \approx \tilde{\rho}_S^I(t)$ in Eq. (A4), and transform the equation of motion back into Schrödinger picture,

$$\begin{aligned} \frac{d}{dt}\tilde{\rho}_S(t) &= -i[\tilde{H}_{0S}, \tilde{\rho}_S(t)] - \int_0^\infty dt' \text{Tr}_B \\ &\times [\tilde{H}_I(t), [e^{-i\tilde{H}_{0S}t'} \tilde{H}_I(t-t') e^{i\tilde{H}_{0S}t'}, \tilde{\rho}_S(t)\rho_B]]. \end{aligned} \quad (\text{A5})$$

Here, we have replaced the variable τ by $t-t'$ and let the upper limit of the integral go to infinity, which is reliable since the integrand vanishes sufficiently quickly as time increases [23].

At zero temperature, the master equation in Eq. (A5) can be rewritten as

$$\begin{aligned} \frac{d}{dt}\tilde{\rho}_S(t) &= -i[\tilde{H}_{0S}, \tilde{\rho}_S(t)] - \int_0^\infty dt' \sum_k \frac{g_k^2}{4} \{ e^{-i(\omega_k - \omega_L)t'} \sigma_+ e^{-i\tilde{H}_{0S}t'} \sigma_- e^{i\tilde{H}_{0S}t'} \tilde{\rho}_S(t) - e^{-i(\omega_k - \omega_L)t'} e^{-i\tilde{H}_{0S}t'} \sigma_- e^{i\tilde{H}_{0S}t'} \tilde{\rho}_S(t) \sigma_+ \\ &- e^{i(\omega_k - \omega_L)t'} \sigma_- \tilde{\rho}_S(t) e^{-i\tilde{H}_{0S}t'} \sigma_+ e^{i\tilde{H}_{0S}t'} + e^{i(\omega_k - \omega_L)t'} \tilde{\rho}_S(t) e^{-i\tilde{H}_{0S}t'} \sigma_+ e^{i\tilde{H}_{0S}t'} \sigma_- \} \end{aligned} \quad (\text{A6})$$

since $\text{Tr}(b_k^\dagger b_k \rho_B) = 0$. It is not difficult to derive following equations:

$$\begin{aligned} e^{-i\tilde{H}_{0S}t} \sigma_\pm e^{i\tilde{H}_{0S}t} &= \left[\frac{\tilde{\Omega}^2}{2\tilde{\Omega}_R^2} + \frac{1}{4} \left(1 + \frac{\tilde{\delta}}{\tilde{\Omega}_R} \right)^2 e^{\mp i\tilde{\Omega}_R t} + \frac{1}{4} \left(1 - \frac{\tilde{\delta}}{\tilde{\Omega}_R} \right)^2 e^{\pm i\tilde{\Omega}_R t} \right] \sigma_\pm \\ &+ \frac{\tilde{\Omega}}{4\tilde{\Omega}_R} \left[\frac{2\tilde{\delta}}{\tilde{\Omega}_R} - \left(1 + \frac{\tilde{\delta}}{\tilde{\Omega}_R} \right) e^{\mp i\tilde{\Omega}_R t} + \left(1 - \frac{\tilde{\delta}}{\tilde{\Omega}_R} \right) e^{\pm i\tilde{\Omega}_R t} \right] \sigma_z + \frac{\tilde{\Omega}^2}{4\tilde{\Omega}_R^2} (2 - e^{-i\tilde{\Omega}_R t} - e^{i\tilde{\Omega}_R t}) \sigma_\mp. \end{aligned} \quad (\text{A7})$$

Substituting Eqs. (A7) into Eq. (A6), integrating with respect to t' , and assuming

$$\int_0^\infty d\tau \sum_k \frac{g_k^2}{4} e^{\pm i(\omega_k - \omega_L \pm \tilde{\Omega}_R)\tau} \approx \int_0^\infty d\tau \sum_k \frac{g_k^2}{4} e^{\pm i(\omega_k - \omega_L)\tau} \approx \frac{\kappa}{2}, \quad (\text{A8})$$

namely, assuming that the decay rate of a driven two-level system remains constant, we finally obtain the form of the master equation presented in Eq. (12).

APPENDIX B: THE DERIVATION OF THE FLUORESCENCE SPECTRUM

For the fluorescence spectrum, it is sufficient to evaluate the integral (17) in the steady-state limit. In this limit, due to the time-dependent unitary transformations (2) and (10), we have the correlation function

$$g^{(1)}(t, t') = \text{Tr}[R(t)e^{S(t)}\sigma_{\pm}e^{-S(t)}R^{\dagger}(t)\tilde{U}(\tau)R(t')e^{S(t')}\sigma_{\mp}e^{-S(t')}R^{\dagger}(t')\tilde{\rho}_{\text{ss}}\otimes\rho_B\tilde{U}^{\dagger}(\tau)], \quad (\text{B1})$$

where $\tilde{\rho}_{\text{ss}}$ is the steady-state solution for master equation (12), $\tilde{U}(\tau) = \exp(-i\tilde{H}\tau)$, and $\tau = t - t'$. The transform $R(t)e^{S(t)}\sigma_{\pm}e^{-S(t)}R^{\dagger}(t)$ in the correlation function can be expressed in terms of σ_{\pm} and σ_z with time-dependent coefficients,

$$\begin{aligned} R(t)e^{S(t)}\sigma_{\pm}e^{-S(t)}R^{\dagger}(t) &= \frac{1 + \cos\left[\frac{2\Omega}{\omega_L}\zeta \sin(\omega_L t)\right]}{2}\sigma_{\pm}e^{\pm i\omega_L t} + \frac{1 - \cos\left[\frac{2\Omega}{\omega_L}\zeta \sin(\omega_L t)\right]}{2}\sigma_{\mp}e^{\mp i\omega_L t} \mp i\frac{\sin\left[\frac{2\Omega}{\omega_L}\zeta \sin(\omega_L t)\right]}{2}\sigma_z \\ &= \frac{1}{2}\sum_{n \text{ odd}} [(j_n e^{\pm i n \omega_L t} + j_{n+2} e^{\mp i n \omega_L t})\sigma_{\pm} + (j'_n e^{\mp i n \omega_L t} + j'_{n+2} e^{\pm i n \omega_L t})\sigma_{\mp} + (j_{n+1} e^{\mp i n \omega_L t} + j'_{n+1} e^{\pm i n \omega_L t})\sigma_z], \end{aligned} \quad (\text{B2})$$

where the summation is taken over all positive odd integers and the series are defined as

$$j_n = \begin{cases} 1 + J_0\left(\frac{2\Omega}{\omega_L}\zeta\right), & n = 1, \\ J_{n-1}\left(\frac{2\Omega}{\omega_L}\zeta\right), & n \neq 1, \end{cases} \quad (\text{B3})$$

and

$$j'_n = \begin{cases} 1 - J_0\left(\frac{2\Omega}{\omega_L}\zeta\right), & n = 1, \\ -J_{n-1}\left(\frac{2\Omega}{\omega_L}\zeta\right), & n \neq 1. \end{cases} \quad (\text{B4})$$

When calculating the spectrum, according to Ref. [24], we approximate the integral by

$$\begin{aligned} I(\omega) &= \lim_{T \rightarrow \infty} \frac{1}{T} \int_0^T dt \int_0^T dt' e^{i n \omega_L t - i m \omega_L t'} \langle \sigma_{\mu}(\tau) \sigma_{\nu}(0) \rangle_s e^{-i\omega(t-t')} \\ &= \lim_{T \rightarrow \infty} \frac{1}{T} \int_0^T dt \int_0^T dt' e^{i n \omega_L \tau - i(m-n)\omega_L t'} \langle \sigma_{\mu}(\tau) \sigma_{\nu}(0) \rangle_s e^{-i\omega\tau} \\ &= \lim_{T \rightarrow \infty} \frac{1}{T} \int_0^T dt' e^{-i(m-n)\omega_L t'} \int_{-t'}^{T-t'} d\tau \langle \sigma_{\mu}(\tau) \sigma_{\nu}(0) \rangle_s e^{i(n\omega_L - \omega)\tau} \\ &= \lim_{T \rightarrow \infty} \frac{1}{T} \int_0^T dt' e^{-i(m-n)\omega_L t'} \int_{-\infty}^{+\infty} d\tau \langle \sigma_{\mu}(\tau) \sigma_{\nu}(0) \rangle_s e^{i(n\omega_L - \omega)\tau} \\ &= \delta_{m,n} \int_{-\infty}^{+\infty} d\tau \langle \sigma_{\mu}(\tau) \sigma_{\nu}(0) \rangle_s e^{i(n\omega_L - \omega)\tau}, \end{aligned} \quad (\text{B5})$$

where $\langle \sigma_{\mu}(\tau) \sigma_{\nu}(0) \rangle_s = \text{Tr}[\sigma_{\mu}(\tau) \sigma_{\nu}(0) \tilde{\rho}_{\text{ss}} \rho_B]$, ($\mu, \nu = +, -, z$). Using this approximation, one can easily show that the spectrum is given by

$$\begin{aligned} S(\omega) &= \frac{1}{4\pi} \text{Re} \sum_{n \text{ odd}} \int_0^{\infty} d\tau e^{-i\omega\tau} [(j_n^2 e^{i n \omega_L \tau} + j_{n+2}^2 e^{-i n \omega_L \tau}) \langle \sigma_{+}(\tau) \sigma_{-}(0) \rangle_s + (j'_n j_{n+2} e^{-i n \omega_L \tau} + j_n j'_{n+2} e^{i n \omega_L \tau}) \langle \sigma_{-}(\tau) \sigma_{-}(0) \rangle_s \\ &\quad + (j_{n+1} j_{n+2} e^{-i n \omega_L \tau} + j_n j'_{n+1} e^{i n \omega_L \tau}) \langle \sigma_z(\tau) \sigma_{-}(0) \rangle_s + (j_n j'_{n+2} e^{i n \omega_L \tau} + j'_n j_{n+2} e^{-i n \omega_L \tau}) \langle \sigma_{+}(\tau) \sigma_{+}(0) \rangle_s \\ &\quad + (j_n^2 e^{-i n \omega_L \tau} + j_{n+2}^2 e^{i n \omega_L \tau}) \langle \sigma_{-}(\tau) \sigma_{+}(0) \rangle_s + (j'_n j_{n+1} e^{-i n \omega_L \tau} + j'_{n+1} j'_{n+2} e^{i n \omega_L \tau}) \langle \sigma_z(\tau) \sigma_{+}(0) \rangle_s \\ &\quad + (j_n j'_{n+1} e^{i n \omega_L \tau} + j_{n+1} j_{n+2} e^{-i n \omega_L \tau}) \langle \sigma_{+}(\tau) \sigma_z(0) \rangle_s + (j'_n j_{n+1} e^{-i n \omega_L \tau} + j'_{n+1} j'_{n+2} e^{i n \omega_L \tau}) \langle \sigma_{-}(\tau) \sigma_z(0) \rangle_s \\ &\quad + (j_{n+1}^2 e^{-i n \omega_L \tau} + j'_{n+1}{}^2 e^{i n \omega_L \tau}) \langle \sigma_z(\tau) \sigma_z(0) \rangle_s], \end{aligned} \quad (\text{B6})$$

where $\text{Re}(z)$ gives the real part of complex number z .

To obtain the explicit expression for the spectrum, it is necessary to evaluate the correlation function $\langle \sigma_{\mu}(\tau) \sigma_{\nu}(0) \rangle_s$, which is evaluated based on quantum regression theorem [26]. Notice that the dynamics of the quantity $\langle \sigma_{\mu}(\tau) \rangle = \langle \sigma_{\mu}(\tau) \rangle - \langle \sigma_{\mu} \rangle_s$ is determined by the homogeneous part of Bloch equations (13). Using quantum regression theorem, we obtain a close set of

differential equations for the quantity $\langle\langle\sigma_\mu(\tau)\sigma_\nu(0)\rangle\rangle = \langle\sigma_\mu(\tau)\sigma_\nu(0)\rangle_s - \langle\sigma_\mu\rangle_s\langle\sigma_\nu\rangle_s$, which is

$$\frac{d}{d\tau}\langle\langle\sigma_\mu(\tau)\sigma_\nu(0)\rangle\rangle = \sum_\lambda M_{\mu\lambda}\langle\langle\sigma_\lambda(\tau)\sigma_\nu(0)\rangle\rangle, \quad (\text{B7})$$

$$M = \begin{pmatrix} -\frac{\kappa}{2} + i\tilde{\delta} & 0 & -i\frac{\tilde{\Omega}}{2} \\ 0 & -\frac{\kappa}{2} - i\tilde{\delta} & i\frac{\tilde{\Omega}}{2} \\ -i\tilde{\Omega} & i\tilde{\Omega} & -\kappa \end{pmatrix}. \quad (\text{B8})$$

One can obtain the following Laplace transforms without difficulty:

$$g_{+v}(p) = \int_0^\infty d\tau e^{-p\tau} \langle\langle\sigma_+(\tau)\sigma_v(0)\rangle\rangle = \frac{\tilde{\Omega}^2(x_{0v} + y_{0v}) - i\tilde{\Omega}z_{0v}(p + i\tilde{\delta} + \frac{\kappa}{2}) + x_{0v}(p + \kappa)(2p + 2i\tilde{\delta} + \kappa)}{2f(p)}, \quad (\text{B9})$$

$$g_{-v}(p) = \int_0^\infty d\tau e^{-p\tau} \langle\langle\sigma_-(\tau)\sigma_v(0)\rangle\rangle = \frac{\tilde{\Omega}^2(x_{0v} + y_{0v}) + i\tilde{\Omega}z_{0v}(p - i\tilde{\delta} + \frac{\kappa}{2}) + y_{0v}(p + \kappa)(2p - 2i\tilde{\delta} + \kappa)}{2f(p)}, \quad (\text{B10})$$

$$g_{zv}(p) = \int_0^\infty d\tau e^{-p\tau} \langle\langle\sigma_z(\tau)\sigma_v(0)\rangle\rangle = \frac{\tilde{\Omega}(x_{0v} + y_{0v})\tilde{\delta} + z_{0v}[\tilde{\delta}^2 + (p + \frac{\kappa}{2})^2] - i\tilde{\Omega}(p + \frac{\kappa}{2})(x_{0v} - y_{0v})}{f(p)}, \quad (\text{B11})$$

where

$$f(p) = p^3 + 2\kappa p^2 + \left(\tilde{\Omega}^2 + \tilde{\delta}^2 + \frac{5}{4}\kappa^2\right)p + \kappa\left(\frac{\tilde{\Omega}^2}{2} + \tilde{\delta}^2 + \frac{\kappa^2}{4}\right) \quad (\text{B12})$$

and

$$x_{0v} = \langle\langle\sigma_+(0)\sigma_v(0)\rangle\rangle, \quad (\text{B13})$$

$$y_{0v} = \langle\langle\sigma_-(0)\sigma_v(0)\rangle\rangle, \quad (\text{B14})$$

$$z_{0v} = \langle\langle\sigma_z(0)\sigma_v(0)\rangle\rangle \quad (\text{B15})$$

are the initial conditions. These results lead to the solutions

$$\langle\langle\sigma_\mu(\tau)\sigma_\nu(0)\rangle\rangle = \sum_{l=1}^3 R_{\mu,l}^{(\nu)} e^{s_l \tau}. \quad (\text{B16})$$

Here, $R_{\mu,l}^{(\nu)} = \lim_{p \rightarrow s_l} (p - s_l)g_{\mu\nu}(p)$, and s_l denotes the three roots for $f(p) = 0$. Consequently, the fluorescence spectrum can be completely determined.

-
- [1] B. R. Mollow, *Phys. Rev.* **188**, 1969 (1969).
[2] R. E. Grove, F. Y. Wu, and S. Ezekiel, *Phys. Rev. A* **15**, 227 (1977).
[3] X. Xu, B. Sun, P. R. Berman, D. G. Steel, A. S. Bracker, D. Gammon, and L. J. Sham, *Science* **317**, 929 (2007).
[4] A. Muller, E. B. Flagg, P. Bianucci, X. Y. Wang, D. G. Deppe, W. Ma, J. Zhang, G. J. Salamo, M. Xiao, and C. K. Shih, *Phys. Rev. Lett.* **99**, 187402 (2007).
[5] S. Ates, S. M. Ulrich, S. Reitzenstein, A. Löffler, A. Forchel, and P. Michler, *Phys. Rev. Lett.* **103**, 167402 (2009).
[6] E. B. Flagg, A. Muller, J. W. Robertson, S. Founta, D. G. Deppe, M. Xiao, W. Ma, G. J. Salamo, and C. K. Shih, *Nat. Phys.* **5**, 203 (2009).
[7] A. N. Vamivakas, Y. Zhao, C. Y. Lu, and M. Atatüre, *Nat. Phys.* **5**, 198 (2009).
[8] S. M. Ulrich, S. Ates, S. Reitzenstein, A. Löffler, A. Forchel, and P. Michler, *Phys. Rev. Lett.* **106**, 247402 (2011).
[9] A. Ulhaq, S. Weiler, S. M. Ulrich, R. Roßbach, M. Jetter, and P. Michler, *Nat. Photonics* **6**, 238 (2012).
[10] G. Wrigge, I. Gerhardt, J. Hwang, G. Zumofen, and V. Sandoghdar, *Nat. Phys.* **4**, 60 (2008).
[11] O. Astafiev, A. M. Zagoskin, A. A. Abdumalikov, Yu. A. Pashkin, T. Yamamoto, K. Inomata, Y. Nakamura, and J. S. Tsai, *Science* **327**, 840 (2010).
[12] A. Moelbjerg, P. Kaer, M. Lorke, and J. Mork, *Phys. Rev. Lett.* **108**, 017401 (2012).

- [13] D. P. S. McCutcheon and A. Nazir, *Phys. Rev. Lett.* **110**, 217401 (2013).
- [14] D. E. Browne and C. H. Keitel, *J. Mod. Opt.* **47**, 1307 (2000).
- [15] P. Forn-Díaz, J. Lisenfeld, D. Marcos, J. J. García-Ripoll, E. Solano, C. J. P. M. Harmans, and J. E. Mooij, *Phys. Rev. Lett.* **105**, 237001 (2010).
- [16] J. Tuorila, M. Silveri, M. Sillanpää, E. Thuneberg, Y. Makhlin, and P. Hakonen, *Phys. Rev. Lett.* **105**, 257003 (2010).
- [17] Q. H. Chen, T. Liu, Y. Y. Zhang, and K. L. Wang, *Europhys. Lett.* **96**, 14003 (2011).
- [18] Q. H. Chen, Y. Yang, T. Liu, and K. L. Wang, *Phys. Rev. A* **82**, 052306 (2010).
- [19] F. Grossmann, T. Dittrich, P. Jung, and P. Hänggi, *Phys. Rev. Lett.* **67**, 516 (1991).
- [20] Z. G. Lü and H. Zheng, *Phys. Rev. A* **86**, 023831 (2012).
- [21] M. Grifoni and P. Hänggi, *Phys. Rep.* **304**, 229 (1998).
- [22] S. Ashhab, J. R. Johansson, A. M. Zagoskin, and F. Nori, *Phys. Rev. A* **75**, 063414 (2007).
- [23] W. H. Louisell, *Quantum Statistical Properties of Radiation* (Wiley, New York, 1973).
- [24] M. O. Scully and M. S. Zubairy, *Quantum Optics* (Cambridge University Press, Cambridge, UK, 1997).
- [25] F. I. Gauthey, C. H. Keitel, P. L. Knight, and A. Maquet, *Phys. Rev. A* **55**, 615 (1997).
- [26] M. Lax, *Phys. Rev.* **172**, 350 (1968).